Perfect invisibility cloaking by isotropic media

T. Xu,[1] Y. C. Liu,[1] Y. Zhang,[1] C. K. Ong,[2] and Y. G. Ma[1,2,*]

[1]*Center for Optical and Electromagnetic Research, State Key Lab of Modern Optical Instrumentation, Department of Optical Engineering, Zhejiang University, Hangzhou 310058, China*

[2]*Center for Superconducting and Magnetic Materials, Department of Physics, National University of Singapore, 2 Science Drive 3, Singapore 117542, Singapore*

(Received 29 July 2012; published 17 October 2012)

In this paper the authors report that perfect invisibility cloaking could be achieved in a medium designed by a non-Euclidean conformal transformation. Wave behaviors could be controlled as well as the cloaking device configured by the general Euclidean approach dealing with the full Maxwell's equations. The cloaking medium proposed here is totally isotropic and can work in waves without the geometry and polarization limits; thus it is very promising for applications to build a device to hide large objects.

DOI: 10.1103/PhysRevA.86.043827 PACS number(s): 42.25.Fx, 42.30.Va, 43.20.+g

Research in invisibility cloaking using metamaterials has grown rapidly after the two celebrated papers by Pendry *et al*. [1] and Leonhardt [2] employing transformation optics (TO). These two approaches were mathematically different in the initial examples and gave cloaks of different index profiles. Pendry's approach is based on wave optics dealing with Maxwell's equations and thus is applicable to the transforms with any situations in a Euclidean space, but as a result it requires very complex cloaking structures with inhomogeneous and anisotropic material properties [1,3–6]. Leonhardt's approach works under geometrical optics dealing with scalar Helmholtz equations and thus is applicable to the transforms of very large structures satisfying adiabatic conditions. It involves curved space transformation, so called non-Euclidean transformation. This non-Euclidean conformal transformation leads to a pure isotropic cloak and yet non-experimental realization appears. Research efforts in the past years have been mainly focused on the general approach and have tried to improve the practical feasibilities with modified algorithms [7,8] and demonstrated the cloaking effect from microwave to visible light [9–16]. But there is still room for theoretical and experimental cloaking-related research to advance in order to reach or at least approach the final aim of practical applications, in particular cloaking objects in full electromagnetic space with no polarization limit.

The non-Euclidean conformal transformation enabling adoption of isotropic cloaks is promising to fulfill this goal and will receive more attention, but in a recent review article conformal mapping was claimed not able to generate real cloaking without suffering internal backscattering that would make the cloak itself visible [17]. This problem has been solved by including the non-Euclidean part to complete the device within the valid range of geometrical optics resorting to internal constructive light interference [18]. In the current paper we will continue to show that the conformal cloaking device can be properly configured to work perfectly for geometric rays and even perfectly for waves. To do this we need to avoid any internal discontinuity reflection and balance the phase difference for lights traveling along different lines. An inside-out Eaton lens, as first proposed by Miñano [19], is incorporated to yield an isotropic cloak that produces a smooth refractive index profile. Negative index materials are introduced in the cloaking core to cancel out the phase delay and provide perfect wave cloaking.

We first briefly recall the conformal transformation technique for cloaking. This technique is generally based on a coordinate mapping from a non-Euclidean virtual space (w) into a planar physical space (z). The non-Euclidean space employed, as shown in Fig. 1(a), consists of two Riemann sheets connected through a branch cut (yellow lines). On the upper sheet the incident light rays (short red arrows) touching the cut line will be refracted onto the lower sheet and guided back onto the upper sheet again by forming a closed loop trajectory. This can be realized by placing a special focusing lens on the lower sheet such as an Eaton lens [2]. The region outside the lens on the lower sheet is optically screened and thus objects placed there are invisible to an observer standing far away on the upper Riemann sheet. This optical process can be transformed into a two-dimensional physical space to generate an invisibility cloak through a conformal mapping. The simple Zhukovsky transform is often used to configure the mapping process, i.e.,

$$w = z + \frac{a^2}{z}, \tag{1}$$

where the constant a, equal to one fourth of the cut line length, determines the final dimension of the cloaking device. One can see $w(z)$ is an analytical function and differentiable by any order, thus satisfying the Cauchy-Riemann conditions for a conformal mapping [3]. Through Eq. (1) the upper (lower) Riemann sheet is mapped to be the region outside (inside) a circle of radius a in the physical space, thus also called the exterior (interior) Riemann sheet [2,18]. The isotropic cloak index profile is calculated by

$$n(z) = \left|\frac{dw}{dz}\right| n', \tag{2}$$

where n' represents the index profile of the original virtual space. The upper sheet is often assumed to be empty space with $n' = 1$ and then the proper choice of n' for the lower sheet is important and it determines the final cloaking performance.

*Corresponding author: yungui@zju.edu.cn

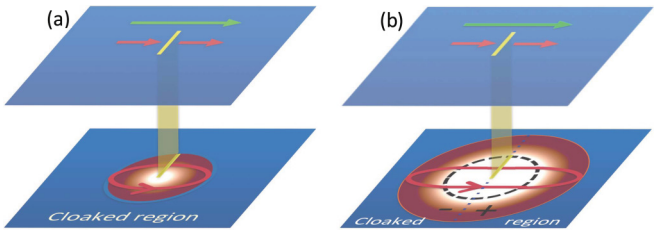

FIG. 1. (Color online) Schematic of the virtual space. It consists of two Riemann sheets with the upper one empty for air and the lower one placed with a usual Eaton lens in (a) and an inside-out Eaton lens in (b). On the upper sheet the incident light rays (short red arrows) heading toward the branch cut (yellow lines) will fall off onto the lower sheet and one loop later travel back onto the upper again. The long green arrows represent light rays not entering the lower sheet. Their interference with the light back from the lower sheet affects the performance of the whole device. Note the cloaking medium in (a) is pure dielectric but has equal magnetic and dielectric values in (b) for the bottom lens consisting of one negative (−) and one positive (+) half.

Here we first use a usual Eaton with the index profile $n' = \sqrt{R/r' - 1}$, with $R = 8a$ and $r' = |w - i2a|$. Outside the Eaton lens n' can take any value since no light enters there. In our simulation it is filled by a perfectly conducting metal. For this configuration internal backscattering will occur once light hits the cut line due to the local impedance mismatch, but this interface scattering will be minimized at certain wavelengths where internal resonance is excited. The Eaton lens belongs to one category of absolute optical instruments that can be conformally constructed by mappings from non-Euclidean geometries [19]. In the optical-mechanical analogy the index profile of the Eaton lens corresponds to a Kepler potential and light propagating inside it will form closed trajectories [20]. Electromagnetically it behaves as a Fabry-Perot waveguide that will induce a phase delay (Φ) in one round of light travel. Constructive interference will happen at some discrete wavelengths satisfying $\Phi = n\pi$ with n an integer and improve the cloaking effect by suppressing internal reflection, as recently discussed by Chen *et al.* [18]. These series wavelengths were further analyzed to correspond to the harmonic eigenmodes of the Eaton lens described by $\lambda = 2\pi R/(2l + 1)$ with the integer l denoting the mode order. We examined these eigenmode conditions and found that they indeed led to perfect wave cloaking but only for some limit cases at $l \leqslant 3$.

Figures 2(a) and 2(b) give the snapshots of the wave patterns through a cloak at two Eigenmodes corresponding to $l = 2$ and 40, respectively. The incident wave comes from the left side and the wave pattern is simulated by COMSOL Multiphysics. The field intensity is normalized by the intensity of the incident wave. Note that although conformal mapping usually yields infinitely large samples, they can be effectively truncated to have finite physical sizes through proper index approximation. Here we define the cloak to have a total radius of $5a$. As shown in Fig. 2(a), good wave cloaking behavior is obtained for $l = 2$ except for slight wave-front deformation. Things placed inside the black hole near the center are invisible. But for $l = 40$, as shown in Fig. 2(b), the same index structure on the contrary causes strong side scattering thus yielding a bad cloaking.

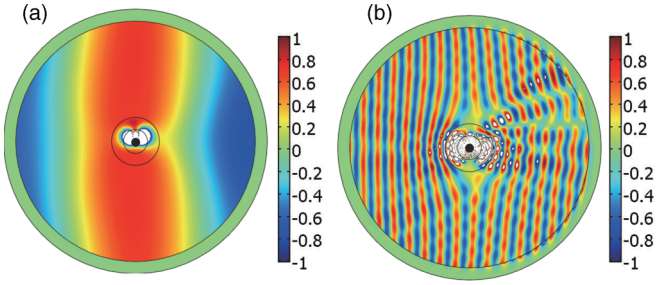

FIG. 2. (Color online) Cloaking effect with an Eaton lens incorporated. An Eaton lens is placed in the lower sheet to guide back the incident light rendering the region outside cloaked as represented by the black holes. The wave patterns in (a) and (b) are the snapshots corresponding to the harmonic eigenmodes of the Eaton lens at the order $l = 2$ and 40, respectively. The wave is denoted by the magnetic component normalized by the incident field.

Similar wave patterns are observed for all the eigenmodes with $l > 3$. This conflicting result cannot be interpreted from the above theory. In addition we also notice that the backscattering is not serious at the Eaton lens's eigenwavelengths. This indicates constructive wave interference does happen inside the inner core of the cloak. But this alone does not grant the cloaking performance because the out-of-phase interference can happen outside the core between the light entering and not entering the core (long green arrows in Fig. 1).

The phase change for light across the cloak core cannot be predicted from geometrical optics, in particular considering a wide incident angle. But in practice we can always choose a lens with continuous boundary conditions and thus avoid internal scattering. Here we choose a modified version of the Eaton lens with the index profile defined by $n' = \sqrt{R/r' - 1}$ at $r' \in [R/2, R]$ and 1 at $r' \in [0, R/2]$, also called the inside-out Eaton lens [19,21,22]. This modified version still possesses the same light refraction characteristics as the original one. In this case light on the upper Riemann sheet will smoothly transfer onto the lower sheet and then be smoothly refracted back to the upper sheet, as shown in Fig. 1(b), without causing any boundary scattering only if the branch cut line is shorter than $R/2$. Undoubtedly this cloak should work perfectly for rays. We examined this characteristic and the wave pattern (not shown here) is found to be very similar to that shown in Fig. 2(b) at the same l. Thus it once again confirms our argument that the out-of-phase interference on the upper Riemann sheet distorts the planar wave fronts near the core edges and causes the unwanted side scattering. For larger samples or at smaller wavelengths the edge influence will be alleviated and acceptable cloaking performance can be anticipated for most of the incident light.

It will still be interesting to inspect whether a conformal cloak can work perfectly for waves with no limit and thus could compete with an anisotropic counterpart designed by the general Euclidean approach. From the pictures in Fig. 1, we know that a usual conformal cloak fails to work for waves due to the retardation of light traveling inside the inner core. Ideal wave cloaking can happen only if this phase delay is made to be zero. For this purpose hereafter we introduce negative index materials and divide the inside-out Eaton lens into two equal halves, e.g., the left half with negative index and the right

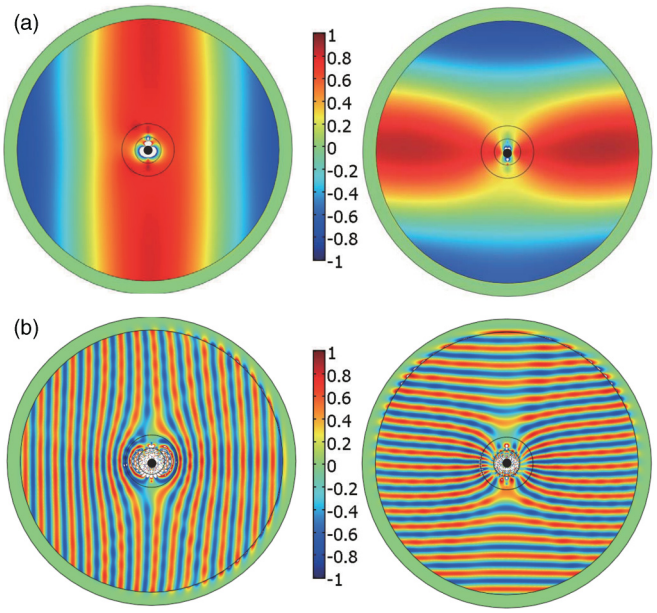

FIG. 3. (Color online) Cloaking effect with an inside-out positive-negative Eaton lens incorporated. The wave patterns in (a) and (b) are simulated at wavelengths corresponding to the Eaton lens's harmonic order $l = 2$ and 4, respectively. In each group, the right (left) figure represents the wave incident from the left (bottom) side. The inside-out Eaton lens with half negative and half positive is employed here to cancel out the phase delay in the inner cloak core.

half with positive index, as schematically shown in Fig. 1(b). Flowing into this composite lens light rays can still form closed loop trajectories but half in the positive region and half in the negative region. As a result the total optical length or phase delay is added to be zero no matter what the incident angle is [23]. This idea is confirmed by the simulation as shown in Figs. 3(a) and 3(b) for $l = 4$ and 40, respectively. In each row, the left (right) figure represents light illumination from the left (bottom) side. Compared with the wave patterns in Figs. 2(a) and 2(b), the wave-front restoration capability after the cloaked shell at both wavelengths is clearly improved, especially for the shorter wavelength at which the strong side scattering is totally suppressed. The observed minor scattering could arise from the regions near the two ends of the branch cut where splitting of light waves may raise certain scattering. This is somehow similar to the phenomenon of inevitable backscattering at the exact center of an ideal anisotropic cloak designed by the general approach [1,3]. The term "perfect" used in this paper does not strictly regard the final performance but more emphasizes its important enhancement since it has been generally accepted that there is no real perfect cloaking. In addition, the quickly increased refractive index values near the cloaked region will cause a technical difficulty in correctly approximating these parts by extremely small simulation meshes. This technical error becomes more serious at short wavelengths and affects the numerical accuracy and the final cloaking effect.

The concept of conformal cloaking was initially introduced under the geometrical optics conditions that require that the local index vary much slower than the operating wavelength, thus corresponding to very large devices [2]. Embedding the inside-out gradient-indexed Eaton lens can remove the internal boundary scattering. But it is still an open question how the wave cloaking will be at different wavelengths, especially

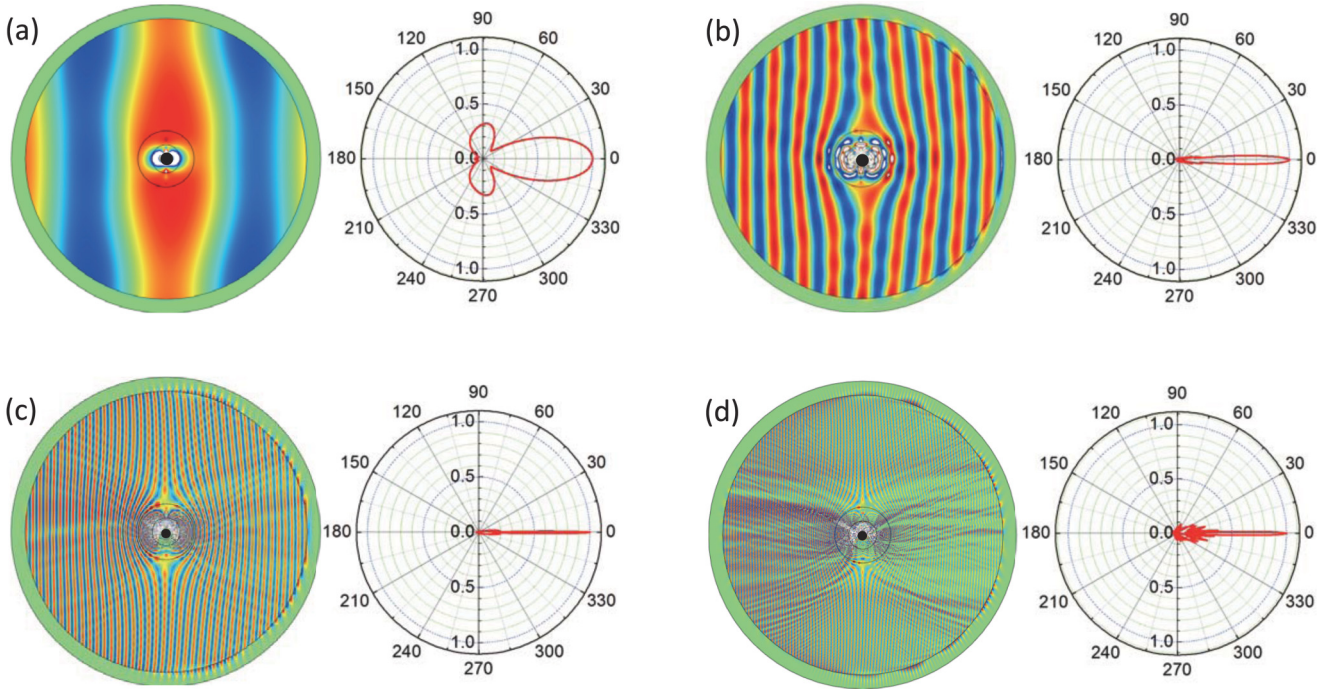

FIG. 4. (Color online) Cloaking effect of the device at different nonharmonic wavelengths. The cloak parameters are the same as discussed in Fig. 3. The wavelength λ equals $5.5a$ (a), a (b), $0.25a$ (c), and $0.1a$ (d), respectively. In each group the right is the wave picture and the left is the normalized corresponding biscattering figure. For the biscattering curve the polar angle starts from the x axis parallel to the incident wave vector.

where the adiabatic condition is not well satisfied at a nonharmonic mode of the embedded Eaton lens. Figures 4(a)–4(d) plot the snapshots of wave pictures and the corresponding biscattering figures of the cloak device at different wavelengths $\lambda = 5.5a$, a, $0.25a$, and $0.1a$, respectively. Each biscattering curve is normalized by the peak intensity of the far-field radiation field (magnetic component) and the polar angle starts from the x axis parallel to the incident wave vector. These figures show a prominent cloaking effect at different wavelengths. But at the wavelength comparable with the cloak device $5a$, as shown in Fig. 4(a), the biscattering figure does indicate a certain amount of side scattering that leads to a relatively broad angular distribution for the radiated wave. This angular distribution is quickly narrowed at smaller wavelengths, as shown in Figs. 4(b)–4(d). This improvement accords with the enhanced adiabatic conditions generally required by a gradient index lens. Note at the smallest wavelength $0.1a$, as shown in Fig. 4(d), the increased side scattering, as described above, is mainly caused by the numerical error limited by our computation capability and in principal it is reducible by refining the simulation meshes, especially for the center region of the cloak where the refractive index increases to very large values. In our current simulation nearly 2 000 000 mesh elements have been used. Therefore we predict our composite (positive and negative materials incorporated) isotropic cloak should have no wavelength limit regarding practical application.

In Figs. 5(a)–5(c) we check the loss influence on the cloaking behavior at different loss levels for the negative index core. This is essential because negative index material is always fabricated with certain losses. The pictures show the cloaking performance will be deteriorated when the imaginary permittivity and permeability become larger than 0.01. This is a very stringent condition for practical application. Amplification of the field intensity by embedding gain materials is necessary to balance the loss influence, which is another engineering challenge in addition to the fabrication of negative index materials [24].

In conclusion, we have managed to prove that a non-Euclidean conformal cloak in principle can work perfectly for waves without the geometrical and polarization limits. To do this a boundary-matched inside-out Eaton lens was incorporated into the design for the inner cloaking core and then equally divided into two parts of positive and negative refractive indices to cancel out the phase delay. The final device showed an elaborate wave cloaking behavior. This result is

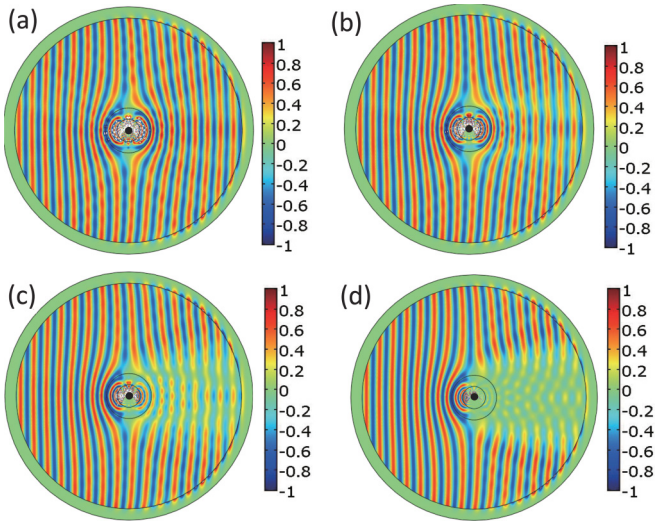

FIG. 5. (Color online) Cloaking effect with loss media. Usage of negative index materials will inevitably involve material loss issues. The inner cloaking cores (the lower Riemann sheet part) in (a)–(d) have imaginary permittivity and permeability of 0, 0.01, 0.03, and 0.1, respectively. One sees that the cloaking performance is very sensitive to signal attenuation.

instrumental and comparable with those designed by a general Euclidean approach considering the full wave equations. Although there could be many challenges for implementation, the conformally designed cloak has its unique advantages and will find important applications when large fabrication is not an issue. The non-Euclidean transformation mathematical approach developed in this paper could be extended to give rise to multiple cloaking cavities, e.g., by introducing multiple virtual Riemann sheets or increasing the number of branch cuts. The same method can also be utilized to create some other interesting devices such as super subwavelength absorbers only if the waves flowing onto the other Riemann sheets can be totally absorbed, which will be reported in the future.

M.Y.G. is partially supported by the NSFC (Grants No. 61271085 and No. 91130004), the Fundamental Research Funds for the Central Universities of China, NCET, and MOE SRFDP of China. Z.Y. is supported by the NSFC (Grants No. 61108022 and No. 60990322). C.K.O. is supported by the Defence Research and Technology Office (DRTech) of Singapore.

[1] J. Pendry, D. Schurig, and D. R. Smith, Science **312**, 1780 (2006).
[2] U. Leonhardt, Science **312**, 1779 (2006).
[3] U. Leonhardt and T. G. Philbin, Prog. Opt. **53**, 69 (2009).
[4] D. Schurig, J. J. Mock, B. J. Justice, S. A. Cummer, J. B. Pendry, A. F. Starr, and D. R. Smith, Science **324**, 977 (2006).
[5] Y. G. Ma, C. K. Ong, T. Tyc, and U. Leonhardt, Nat. Mater. **8**, 639 (2009).
[6] D. R. Smith, J. B. Pendry, and M. C. K. Wiltshire, Science **305**, 788 (2004).
[7] J. S. Li and J. B. Pendry, Phys. Rev. Lett. **101**, 203901 (2008).
[8] U. Leonhardt and T. Tyc, Science **323**, 110 (2009).
[9] J. Valentine, J. S. Li, T. Zentgraf, G. Bartal, and X. Zhang, Nat. Mater. **8**, 568 (2009).
[10] L. H. Gabrielli, J. Cardenas, C. B. Poitras, and M. Lipson, Nat. Photonics **3**, 461 (2009).
[11] R. Liu, C. Ji, J. J. Mock, J. Y. Chin, T. J. Cui, and D. R. Smith, Science **323**, 366 (2009).
[12] T. Ergin, N. Stenger, P. Brenner, J. B. Pendry, and M. Wegener, Science **328**, 337 (2010).
[13] H. F. Ma and T. J. Cui, Nature Commun. **1**, 124 (2010).

[14] X. Z. Chen, Y. Luo, J. J. Zhang, K. Jiang, J. B. Pendry, and S. A. Zhang, Nat. Commun. **2**, 176 (2011).
[15] B. L. Zhang, Y. Luo, X. G. Liu, and G. Barbastathis, Phys. Rev. Lett. **106**, 033901 (2011).
[16] M. Choi, S. H. Lee, Y. Kim, S. B. Kang, J. Shin, M. H. Kwak, K. Y. Kang, Y. H. Lee, N. Park, and B. Min, Nature **470**, 369 (2011).
[17] Y. A. Urzhumov, N. B. Kundtz, D. R. Smith, and J. B. Pendry, J. Opt. **13**, 024002 (2011).
[18] H. Y. Chen, U. Leonhardt, and T. Tyc, Phys. Rev. A **83**, 055801 (2011).
[19] J. C. Miñano, Opt. Express **14**, 9627 (2006).
[20] M. Sarbort and T. Tyc, J. Opt. **14**, 075705 (2012).
[21] U. Leonhardt and T. G. Philbin, *Geometry and Light: The Science of Invisibility* (Dover, Mineola, NY, 2010).
[22] Y. Zeng and D. H. Werner, Opt. Express **20**, 2335 (2012).
[23] T. Ochiai, U. Leonhardt, and J. C. Nacher, J. Math. Phys. **49**, 032903 (2008).
[24] S. M. Xiao, V. P. Drachev, A. V. Kildishev, X. J. Ni, U. K. Chettiar, H. K. Yuan, and V. M. Shalaev, Nature **466**, 735 (2010).